Progress In Electromagnetics Research C, Vol. 105, 175–184, 2020

A Loop Antenna with Enlarged Bandwidth of Circular Polarization — Its Application in a Comb-Line Antenna

Kazuhide Hirose[1, *], Motoshi Nakatsu[1], and Hisamatsu Nakano[2]

Abstract—Using the moment method, we analyze a loop antenna with a perturbation segment in the presence of a ground plane. First, the radiation characteristics versus loop height above the ground plane are investigated. It is found that as the loop height increases to more than 0.2 wavelengths, a novel antenna other than a conventional one can exist, showing an enlarged bandwidth of 9% for a 3 dB axial-ratio criterion. Next, the radiation mechanism of the novel antenna is compared with that of the conventional one. Last, the novel loop is used in a comb-line antenna as a radiation element. It is found that the CP wave bandwidth is five times as wide as that of a conventional comb-line antenna. The analysis results are verified by experimental work.

1. INTRODUCTION

It is known that a loop antenna with a single feed can radiate a circularly polarized (CP) wave when the loop has a reactance loading [1], gap [2], and perturbation segment [3]. The antenna has a simple configuration without any feed network in comparison with that for two feeds. So far, the investigations have been restricted to the case for fixed loop height above the ground plane.

Recently, attention has been paid to antenna characteristics for varied loop height [4]. This paper is a sequel to the preliminary conference paper [4] and demonstrates the newest development of a loop antenna with a perturbation segment. The purpose of this paper is to examine the effects of an increase in the loop height on the radiation characteristics using the moment method [5].

After showing fundamental characteristics for a loop height of 1/8 wavelengths [3], we consider radiation characteristics versus the loop height. There is found to be a novel loop showing a wider CP wave bandwidth than a conventional one. The radiation mechanism of the novel loop is discussed, and the novel loop is applied in a CP comb-line antenna [6–8] as a radiation element. The simulated results are validated by experimental ones. Note that the application in the comb-line antenna has not been investigated in the conference paper [4]. In addition, the radiation mechanism of the novel loop element is discussed for the first time in this paper, together with experimental work on the novel loop element.

2. CONVENTIONAL LOOP ELEMENT AND ANALYSIS METHOD

Figure 1 shows an antenna configuration and coordinate system. A square loop of perimeter P is located at height h above a ground plane. The loop is fed from a corner F via a straight wire F-F$'$ using a coaxial line, as shown in Fig. 1(c). To obtain CP radiation, we add a perturbation segment of length $\Delta\ell$ to the loop [3]. The antenna is made of wires with a radius ρ.

The moment method [5] is used for the antenna analysis. The loop perimeter and perturbation segment length (P, $\Delta\ell$) are selected for CP radiation as a function of loop height h. The wire radius is

Received 19 July 2020, Accepted 8 September 2020, Scheduled 20 September 2020

* Corresponding author: Kazuhide Hirose (khirose@shibaura-it.ac.jp).

[1] College of Engineering, Shibaura Institute of Technology, Tokyo 135-8548, Japan. [2] Science and Engineering, Hosei University, Tokyo 184-8584, Japan.

fixed to be $\rho = \lambda_0/200$ [3, 8], where λ_0 is the free-space wavelength at a test frequency f_0. Note that the ground-plane size is assumed to be infinite, and image theory is used.

In this section, we present the fundamental characteristics of a conventional element with a loop height of $h = \lambda_0/8$ [3, 8]. The analysis shows that when the loop perimeter and perturbation segment length are $(P,\ \Delta\ell) = (0.99\lambda_0,\ 0.13\lambda_0)$, the element radiates a CP wave with an axial ratio of 0.1 dB.

The simulated radiation pattern for $(P,\ \Delta\ell) = (0.99\lambda_0,\ 0.13\lambda_0)$ is shown in Fig. 2. The pattern is shown with right (E_R) and left-hand (E_L) CP wave components. It is seen that a right-hand CP radiation beam is formed in the $+z$-axis direction. The half-power beamwidth (HPBW) is 73°. The gain is evaluated to be 9.0 dB.

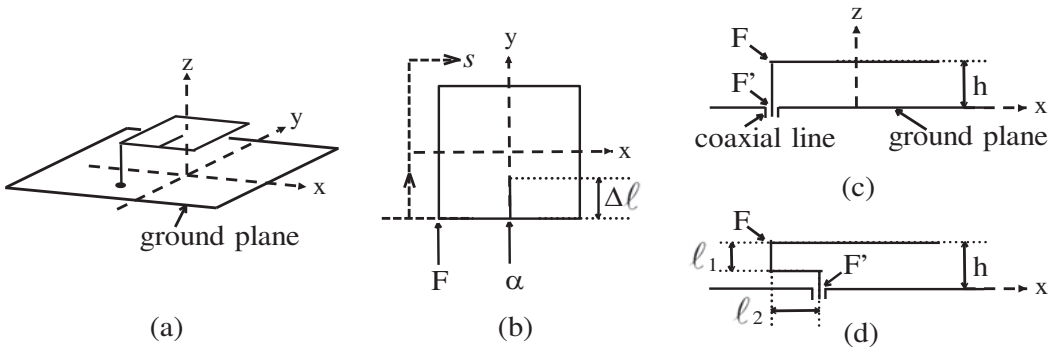

Figure 1. Loop element. (a) Perspective view. (b) Top view. (c) Side view with a straight wire F-F′. (d) Side view with a crank wire F-F′ for impedance matching.

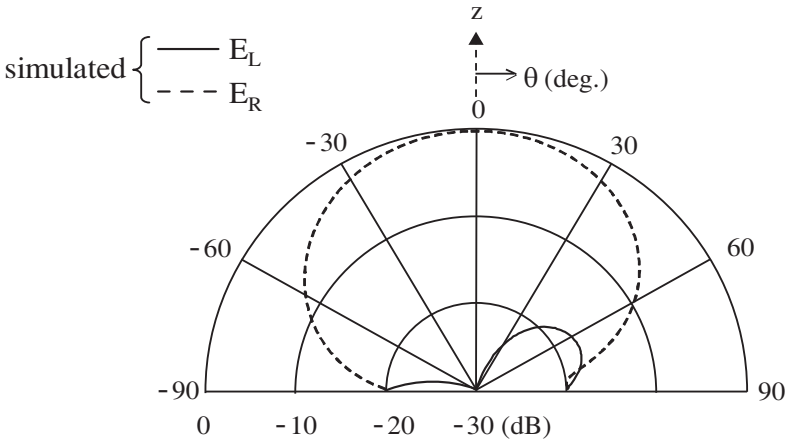

Figure 2. Simulated radiation pattern in $\phi = 0°$ plane for a conventional loop element with $h = \lambda_0/8$.

3. NOVEL LOOP ELEMENT

Now, we consider radiation characteristics versus loop height h, ranging from $\lambda_0/10$ to $\lambda_0/4$. At each value of h, the loop parameters $(P,\ \Delta\ell)$ are optimized for an axial ratio of less than 0.1 dB.

Figure 3 shows the simulated CP wave bandwidth for a 3 dB axial-ratio criterion versus loop height h. It is revealed that as the loop height increases to more than $h = 0.18\lambda_0$, a novel antenna can exist, showing a wider CP bandwidth than a conventional one. A maximum bandwidth of 9.0% is obtained at $h = \lambda_0/4$. Note that the bandwidth of the novel antenna reaches 13% at $h = 0.4\lambda_0$, but the gain decreases by 4 dB compared with that at $h = \lambda_0/4$.

The above-mentioned results are obtained for the straight wire F-F′ shown in Fig. 1(c). To obtain input impedance that matches a 50 Ω coaxial line, we transform the straight wire into a crank one

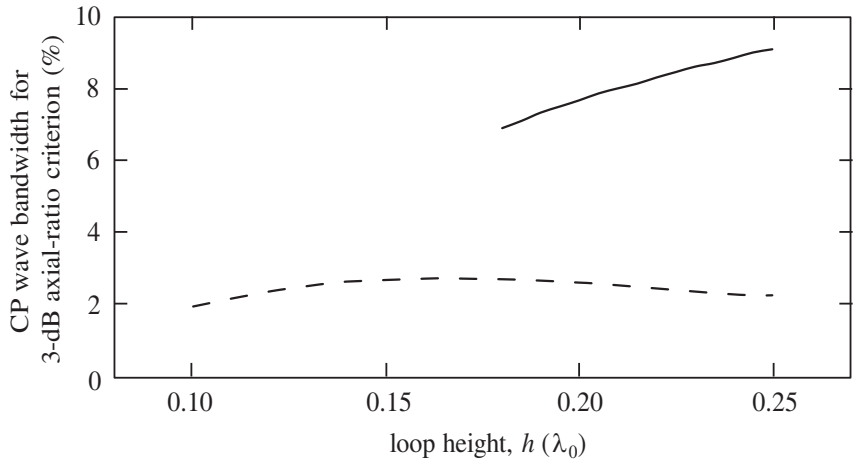

Figure 3. Simulated CP wave bandwidths versus loop height h above the ground plane. The solid and dotted lines show the results of novel and conventional loop elements, respectively Note that at each value of h, the loop parameters are optimized for an axial ratio < 0.1 dB. The solid line vanishes in a range of $h < 0.18\lambda$, since the axial ratio < 0.1 dB is not obtained.

shown in Fig. 1(d). The crank-wire parameters (ℓ_1, ℓ_2) are selected for a VSWR of less than 2 under the condition that the radiation characteristics for the straight wire remain unchanged.

Solid and dotted lines in Fig. 4 show the simulated radiation pattern for $(\ell_1, \ell_2) = (0.23\lambda_0, 0.24\lambda_0)$ and $h = \lambda_0/4$. It is found that the antenna radiates a left-hand CP wave, which is different from that of the conventional element shown in Fig. 2. The HPBW is wider (77°) than that of the conventional element, resulting in a lower gain of 7.2 dB.

The simulated gain, axial ratio, and VSWR versus frequency are shown with solid lines in Fig. 5. The CP wave bandwidth is 8.6%, where the gain and VSWR are more than 6.8 dB and less than 2, respectively.

To verify the simulated results, we fabricate an antenna at $f_0 = 3$ GHz using a ground plane of $5\lambda_0 \times 5\lambda_0$, which is empirically known to be an adequate approximation of the infinite ground plane. The experimental results of the radiation pattern are shown with dots and small circles in Fig. 4. They are in agreement with the simulated results. Agreement between the experimental and simulated results is also found for the frequency responses shown in Fig. 5, where small circles are the experimental results.

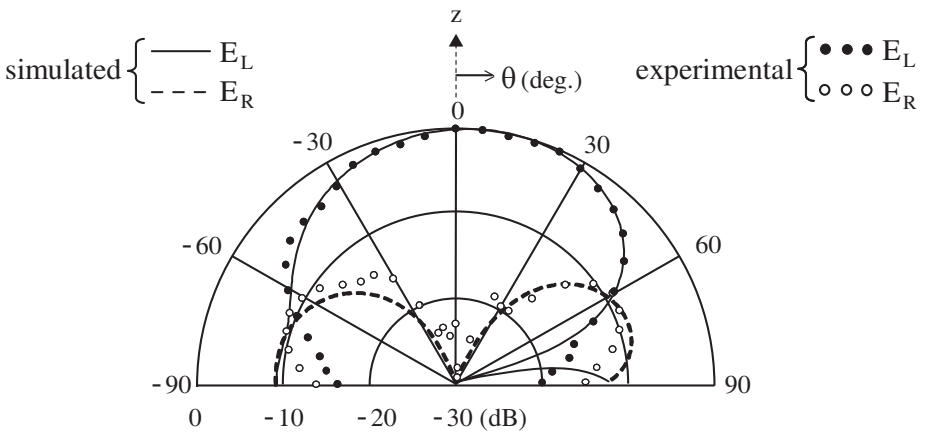

Figure 4. Radiation pattern in $\phi = 0°$ plane for a novel loop element with $h = \lambda_0/4$. The element has loop parameters of $(P, \Delta\ell) = (1.22\lambda_0, 0.23\lambda_0)$ and a crank wire F-F′ for impedance matching [see Fig. 1(d)].

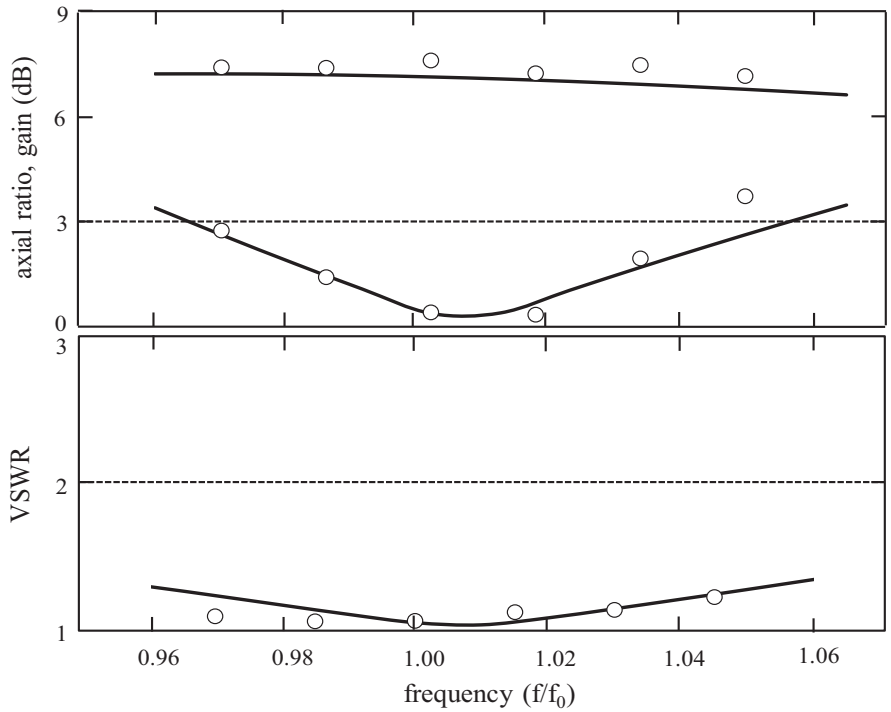

Figure 5. Frequency responses of axial ratio, gain, and VSWR of a novel loop element with $h = \lambda_0/4$. The simulated and experimental results are shown with solid lines and small circles, respectively.

4. RADIATION MECHANISM OF NOVEL LOOP ELEMENT

So far, we have found a novel loop element showing a wider CP wave bandwidth than a conventional one. In this section, the radiation mechanism of the novel element is discussed.

First, we know the reason why the rotational senses of the CP waves of the novel and conventional elements are different from each other. For this, we compare their current distributions shown in Fig. 6. The abscissa is length s, measured from the corner F along the loop clockwise, as shown in Fig. 1(b). Note that a discontinuity of the current occurs at a point α, where the perturbation segment is connected to the loop, as shown in Fig. 1(b).

It is observed from Fig. 6 that as the length s increases, the current phase of the novel loop lags, while the phase of the conventional loop leads. This means that the novel-loop current travels clockwise, radiating a left-hand CP wave in the $+z$-axis direction, while the conventional-loop current radiates a right-hand CP wave. These are consistent with the principal radiation components shown Figs. 4 and 2.

Next, consideration is given to an axial ratio of partial radiation. A comparison between axial ratios for the novel and conventional loop elements are shown in Table 1, where the last row shows an axial

Table 1. Comparison between axial ratios of partial radiation for novel and conventional loop elements.

Partial Radiation	**Axial Ratios**	
	Novel loop element with $h = \lambda_0/4$	**Conventional loop element with $h = \lambda_0/8$**
Loop	6.8 dB	1.6 dB
Loop with PS*	0.1 dB	0.1 dB

PS*: Perturbation segment

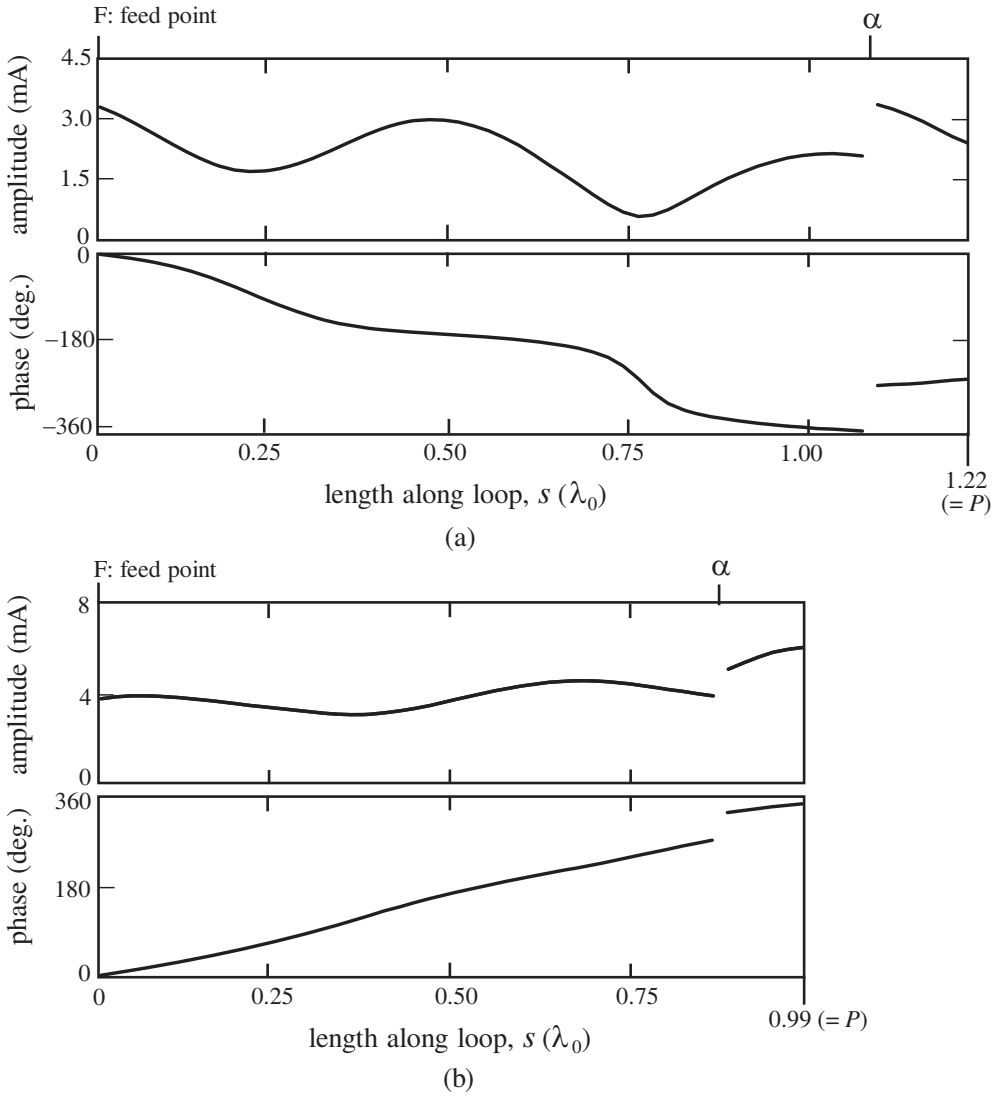

Figure 6. Current distributions along loops. (a) Novel loop element with $h = \lambda_0/4$. (b) Conventional loop element with $h = \lambda_0/8$. Note that loop length, s, of the abscissa is defined in Fig. 1(b).

ratio evaluated using the partial radiation from the loop with a perturbation segment (PS). It is found that the axial ratios from the loops without PS's are 6.8 dB and 1.6 dB for the novel and conventional elements, respectively. This means that partial radiation from the PS for the novel element significantly contributes to a low axial ratio of 0.1 dB (see the last row) than that of the conventional element.

In summary, a difference between the rotational senses of the CP waves of the novel and conventional elements is attributed to opposite directions in which their currents travel along the loops. In addition, partial radiation from the PS in the novel element makes a significant contribution to the low axial ratio, when compared with that for the conventional element.

5. COMB-LINE ANTENNA WITH NOVEL LOOP ELEMENTS

In this section, we use a novel loop in a comb-line antenna [6–8] as a radiation element. The antenna height is taken to be $h = \lambda_0/4$ for the loop to show an enlarged CP wave bandwidth discussed in Section 3. Note that there has been no study of a comb-line antenna operating at $h = \lambda_0/4$, since the radiation characteristics may deteriorate due to unwanted radiation from a coplanar feedline.

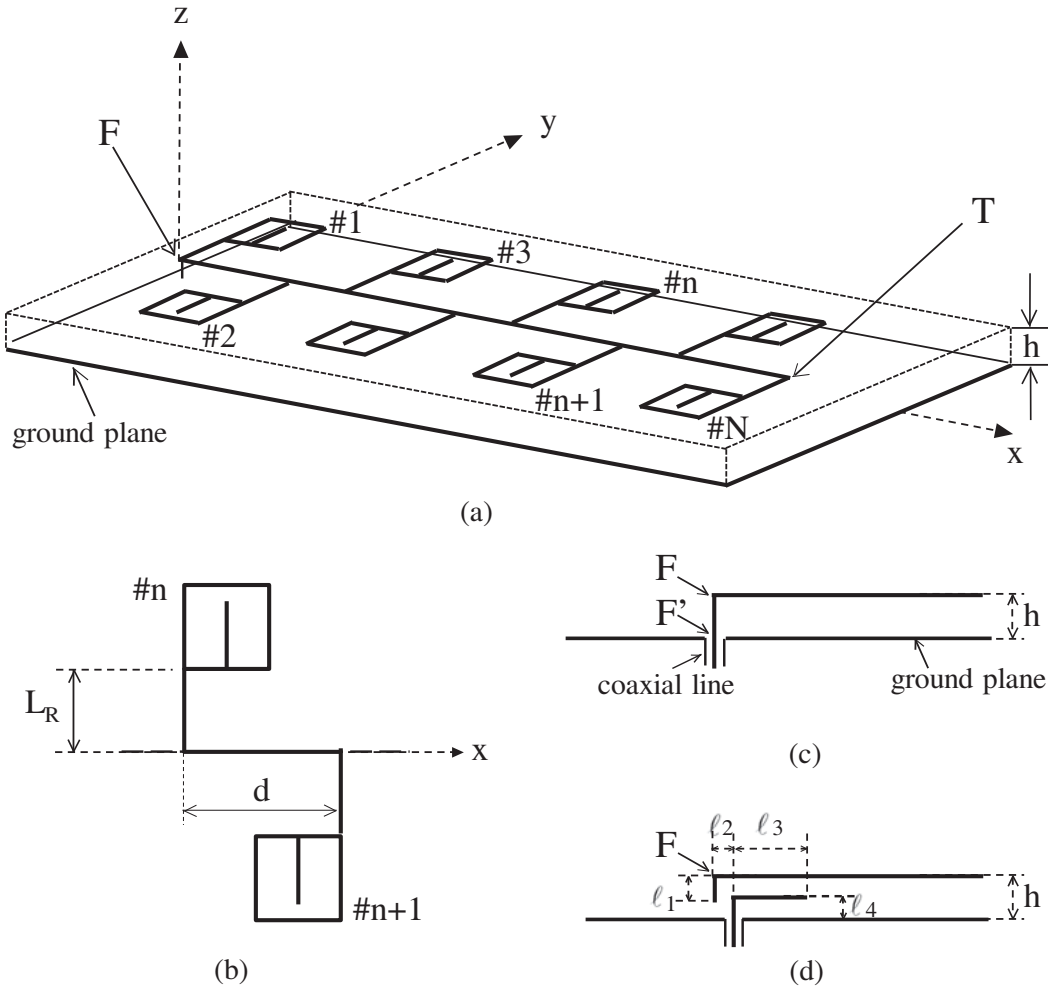

Figure 7. Comb-line antenna with novel loop elements. (a) Perspective view. (b) Top view with elements of #n and $n+1$. (c) Side view with a direct feed using a straight wire F-F′. (d) Side view with an electromagnetic-coupling feed for impedance matching.

Figure 7 shows the antenna configuration. The antenna is located at height h above a ground plane and made of wires with a radius ρ [3, 8]. The comb line is composed of a coplanar feedline F-T above the x axis and straight radiation elements (of length L_R) branching in the $\pm y$ directions. The distance between the radiation elements is designated as d. The feedline F-T is excited at the left end F via a straight wire F-F′ using a coaxial line, as shown in Fig. 7(c) and the right end T is open-circuited. To obtain CP radiation, we add a loop to each tip of the straight radiation element, as shown in Fig. 7(b) [8]. The number of the loops is denoted by N.

The antenna is designed to radiate a CP beam in a direction normal to the antenna plane, in the $+z$-axis direction. For this, we first take the radiation-element distance to be $d = \lambda_0/2$ and rotate the loops on the $+y$ side by 180° with respect to the loops on the $-y$ one to compensate for an excitation phase difference of 180°, as shown in Fig. 7(b). Next, we select the loop parameters (P, $\Delta\ell$) for CP radiation. The other antenna configuration parameters are chosen to be the same as those in [8], $(N, \rho, L_R) = (4, \lambda_0/200, \lambda_0/4)$, to facilitate comparison. Note that an electromagnetic-coupling feed shown in Fig. 7(d) is used for a VSWR of less than 2 [8], and the configuration parameters are empirically determined to be $(\ell_1, \ell_2, \ell_3, \ell_4) = (0.24\lambda_0, 0.02\lambda_0, 0.15\lambda_0, 0.15\lambda_0)$ under the condition that the radiation characteristics for the direct feed shown in Fig. 7(c) remain unchanged.

Calculations show that a CP beam in the $+z$-axis direction is formed for $(d, P, \Delta\ell) = (0.50\lambda_0, 1.13\lambda_0, 0.22\lambda_0)$. The simulated radiation pattern is shown with solid and dotted lines in

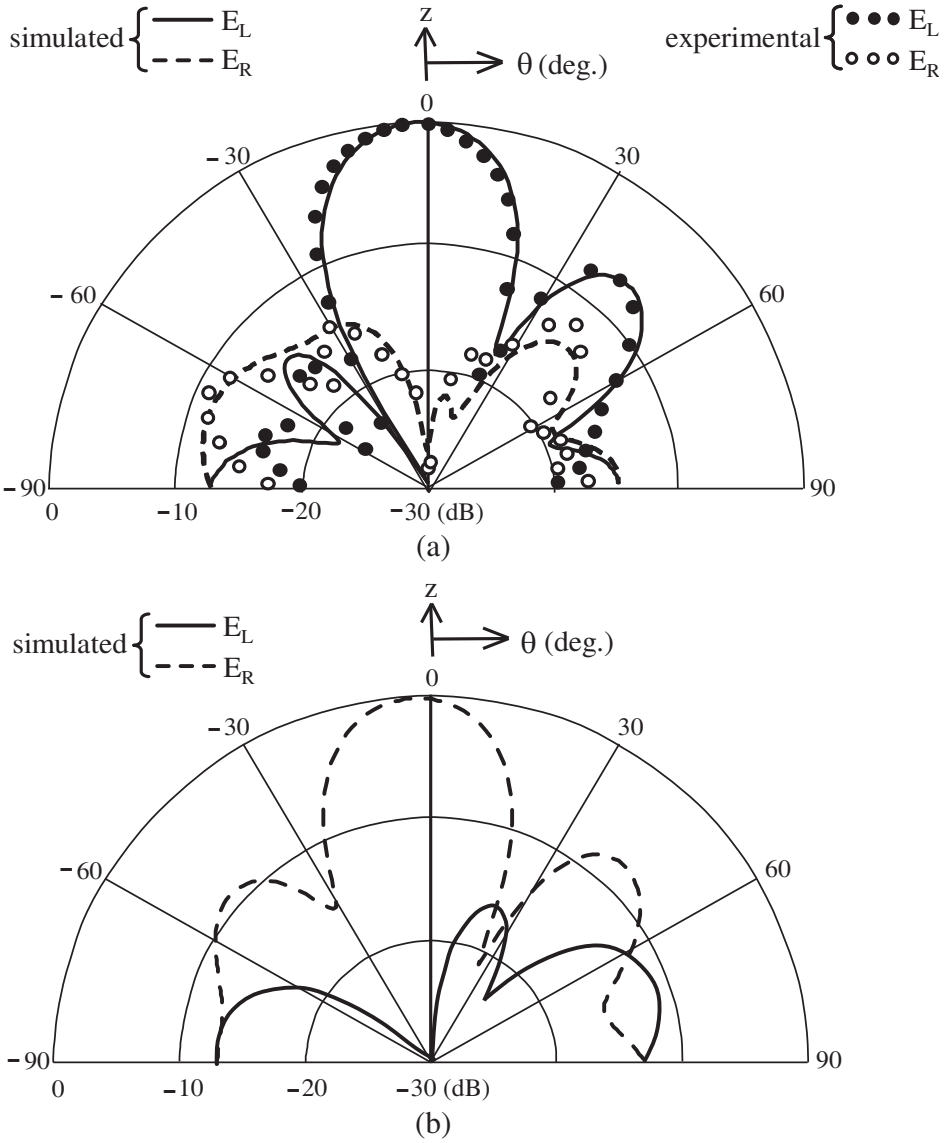

Figure 8. Radiation patterns in $\phi = 0°$ plane for comb-line antennas with $N = 4$. (a) Present antenna with $h = \lambda_0/4$. (b) Conventional antenna with $h = \lambda_0/8$.

Fig. 8(a). The HPWB is 26°, and the gain is 12.1 dB. For comparison, the radiation pattern of a conventional antenna with $h = \lambda_0/8$ [8] is shown in Fig. 8(b). The HPBW and gain are 25° and 12.6 dB, respectively. The gain is higher than that of the present antenna, since the conventional loop element has a higher gain than the novel one, as mentioned in Sections 2 and 3.

The simulated gain and axial ratio of the present antenna versus frequency are shown with solid lines in Fig. 9(a). It is found that the antenna shows a CP wave bandwidth of 7.9%, where the gain is more than 11.3 dB. For comparison, those of the conventional antenna [8] are shown with dotted lines. The CP wave bandwidth is 1.6%. It is emphasized that the bandwidth of the present antenna is five times as wide as that of the conventional one. A solid line in Fig. 9(b) shows the simulated frequency response of the VSWR, which remains less than 2 in the CP wave bandwidth.

To validate the simulated results, we fabricate an antenna at $f_0 = 3$ GHz. Photographs of the fabricated antenna are shown in Fig. 10, where foam material is used for supporting the antenna not to change the radiation characteristics. The experimental results are shown with small circles and dots in Figs. 8(a) and 9. It is seen that the experimental results agree well with the simulated ones.

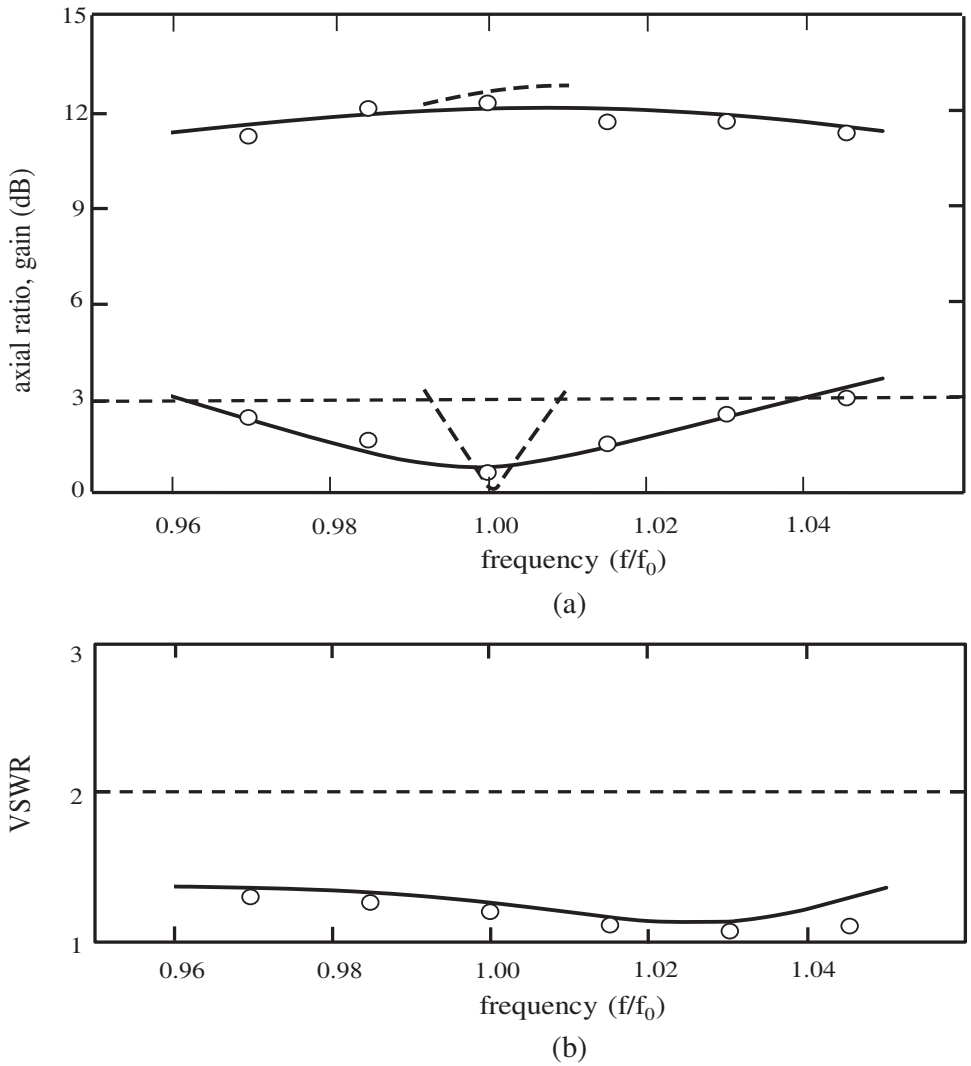

Figure 9. Frequency responses of axial ratio, gain, and VSWR of the present antenna. (a) Axial ratio and gain. (b) VSWR. The solid and small circles show the simulated and experimental results, respectively. For reference, the dotted lines show the simulated results of the conventional antenna. Note that the axial ratio and gain are evaluated in the z-axis direction.

Table 2. Differences between the present and reference [8] studies.

Studies	**Configuration Parameters**		
	Loop height h	**Radiation Element length L_R**	**Number of loops N**
Present	varied (optimized to be $\lambda_0/4$)	fixed ($\lambda_0/4$)	fixed (4)
Reference [8]	fixed ($\lambda_0/8$)	varied (optimized to be $\lambda_0/4$)	reduced from 16 (axial ratio remains unchanged even for a small N, e.g., 4)

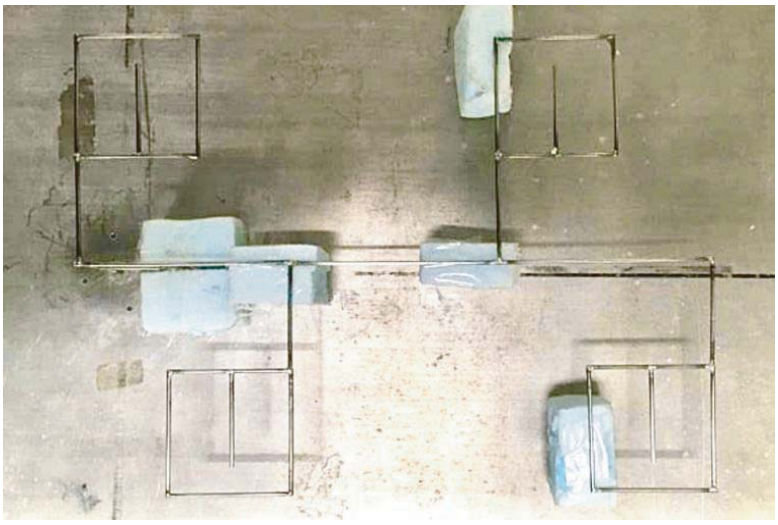

(a)

(b)

Figure 10. Photographs of a comb-line antenna fabricated for experimental work. (a) Top view. (b) Side view.

Finally, we emphasize differences between the present and reference [8] studies. The differences are summarized in Table 2. Loop height h is optimized to enlarge the CP wave bandwidth in the present study, while h is not optimized but fixed in the reference study. Instead, radiation element length L_R is optimized for CP radiation, and the number of loops N is reduced with the other parameters being fixed.

6. CONCLUSION

We have investigated a loop antenna with a perturbation segment to reveal the effects of an increase in loop height on the radiation characteristics. It is found that a novel loop shows a maximum CP wave bandwidth of 9%, while the bandwidth of a conventional loop remains almost unchanged at 3%. It is also found that the rotational senses of the CP waves of the novel and conventional loops are different from each other. After discussing the radiation mechanism of the novel loop, we apply a novel loop in a comb-line antenna as a radiation element. It is found that the CP wave bandwidth is wider than that of a conventional comb-line antenna by a factor of 5. The simulated results are validated by experimental work.

ACKNOWLEDGMENT

The authors would like to thank Blair Thomson for his invaluable assistance in the preparation of this manuscript.

REFERENCES

1. Li, R., N. A. Bushyager, J. Laskar, and M. M. Tentzeris, "Determination of reactance loading for circularly polarized circular loop antennas with a uniform traveling-wave current distribution," *IEEE Trans. Antennas Propag.*, Vol. 53, No. 12, 3920–3929, Dec. 2005.
2. Sumi, M., K. Hirasawa, and S. Shi, "Two rectangular loops fed in series for broadband circular polarization and impedance matching," *IEEE Trans. Antennas Propag.*, Vol. 52, No. 2, 551–554, Feb. 2004.
3. Hirose, K., T. Shibasaki, Y. Yoshida, and H. Nakano, "Ladder antennas for dual circular polarization," *IEEE Antennas Wireless Propag. Lett.*, Vol. 11, 1174–1177, 2012.
4. Hirose, K., K. Okiyama, and H. Nakano, "A loop antennas with wideband circular polarization," *Proc. IEEE Antennas Propag. Society Int. Symp.*, 503–504, 2017.
5. Harrington, R. F., *Field Computation by Moment Methods*, Macmillan, New York, NY, USA, 1968.
6. Zhang, L., W. Zhang, and Y. P. Zhang, "Microstrip grid and comb array antennas," *IEEE Trans. Antennas Propag.*, Vol. 59, No. 11, 4077–4084, Nov. 2011.
7. Cameron, T. R., A. T. Sutinjo, and M. Okoniewski, "A circularly polarized broadside radiating 'herringbone' array design with the leaky-wave approach," *IEEE Antennas Wireless Propag. Lett.*, Vol. 9, 826–829, 2010.
8. Hirose, K., D. Yamada, and H. Nakano, "A modified comb-line antenna radiating a circularly polarized wave," *Trans. IEICE*, Vol. J86-B, No. 10, 2174–2181, Oct. 2003.